Environmental Science and Ecotechnology 20 (2024) 100408

Contents lists available at ScienceDirect

Environmental Science and Ecotechnology

journal homepage: www.journals.elsevier.com/environmental-science-and-ecotechnology/

Original Research

Modifying temperature-related cardiovascular mortality through green-blue space exposure

Kejia Hu [a, b], Shiyi Wang [c], Fangrong Fei [d], Jinglu Song [e], Feng Chen [f], Qi Zhao [g], Yujie Shen [a], Jingqiao Fu [h], Yunquan Zhang [i], Jian Cheng [j], Jieming Zhong [d, 1, *], Xuchao Yang [h, 1, **], Jiayu Wu [c, 1, ***]

[a] School of Public Health, Zhejiang University, Hangzhou, 310058, China
[b] Key Laboratory of Intelligent Preventive Medicine of Zhejiang Province, Hangzhou, 310058, China
[c] College of Agriculture and Biotechnology, Zhejiang University, Hangzhou, 310058, China
[d] Zhejiang Provincial Center for Disease Control and Prevention, Hangzhou, 310051, China
[e] Department of Urban Planning and Design, Xi'an Jiaotong-Liverpool University, Suzhou, 215123, China
[f] Zhejiang Institute of Meteorological Sciences, Hangzhou, 310008, China
[g] School of Public Health, Shandong University, Jinan, 250012, China
[h] Ocean College, Zhejiang University, Zhoushan, 316021, China
[i] School of Public Health, Wuhan University of Science and Technology, Wuhan, 430065, China
[j] School of Public Health, Anhui Medical University, Hefei, 230032, China

ARTICLE INFO

Article history:
Received 3 August 2023
Received in revised form
29 February 2024
Accepted 2 March 2024

Keywords:
Green space
Blue space
Temperature
Mortality
China

ABSTRACT

Green-blue spaces (GBS) are pivotal in mitigating thermal discomfort. However, their management lacks guidelines rooted in epidemiological evidence for specific planning and design. Here we show how various GBS types modify the link between non-optimal temperatures and cardiovascular mortality across different thermal extremes. We merged fine-scale population density and GBS data to create novel GBS exposure index. A case time series approach was employed to analyse temperature-cardiovascular mortality association and the effect modifications of type-specific GBSs across 1085 subdistricts in south-eastern China. Our findings indicate that both green and blue spaces may significantly reduce high-temperature-related cardiovascular mortality risks (e.g., for low (5%) vs. high (95%) level of overall green spaces at 99th vs. minimum mortality temperature (MMT), Ratio of relative risk (RRR) = 1.14 (95% CI: 1.07, 1.21); for overall blue spaces, RRR = 1.20 (95% CI: 1.12, 1.29)), while specific blue space types offer protection against cold temperatures (e.g., for the rivers at 1st vs MMT, RRR = 1.17 (95% CI: 1.07, 1.28)). Notably, forests, parks, nature reserves, street greenery, and lakes are linked with lower heat-related cardiovascular mortality, whereas rivers and coasts mitigate cold-related cardiovascular mortality. Blue spaces provide greater benefits than green spaces. The severity of temperature extremes further amplifies GBS's protective effects. This study enhances our understanding of how type-specific GBS influences health risks associated with non-optimal temperatures, offering valuable insights for integrating GBS into climate adaptation strategies for maximal health benefits.
© 2024 The Authors. Published by Elsevier B.V. on behalf of Chinese Society for Environmental Sciences, Harbin Institute of Technology, Chinese Research Academy of Environmental Sciences. This is an open access article under the CC BY-NC-ND license (http://creativecommons.org/licenses/by-nc-nd/4.0/).

1. Introduction

Cardiovascular diseases (CVDs), including coronary heart disease, stroke, and other heart diseases, remain the leading cause of death in the world [1]. Non-optimum ambient temperature is an important risk factor for CVDs [2]. Globally, CVD mortality burdens attributable to high and low temperatures were estimated at 0.4% and 12.7%, respectively [3]. Over the period from 1990 to 2019, deaths associated with non-optimum temperatures saw a marked

* Corresponding author.
** Corresponding author.
*** Corresponding author.
E-mail addresses: jmzhong@cdc.zj.cn (J. Zhong), yangxuchao@zju.edu.cn (X. Yang), wujiayula@zju.edu.cn (J. Wu).
[1] These authors are co-corresponding authors.

https://doi.org/10.1016/j.ese.2024.100408
2666-4984/© 2024 The Authors. Published by Elsevier B.V. on behalf of Chinese Society for Environmental Sciences, Harbin Institute of Technology, Chinese Research Academy of Environmental Sciences. This is an open access article under the CC BY-NC-ND license (http://creativecommons.org/licenses/by-nc-nd/4.0/).

increase of 45%, with those linked to low temperatures rising by 36% and high temperatures by 600% [4]. These trends will worsen over the next few decades, driven by ongoing climate change, increasing extreme weather events, and population ageing [5,6]. Globally, the temperature-related mortality burden is expected to increase more in low- and middle-income countries, including China [7]. While a range of preparedness and emergency measures and public health guidelines exist in China so far, the need for upscaling interventions exceeds the current capacity of the governance system to prevent temperature-related excess deaths, which calls for innovative and sustainable strategies such as nature-based solutions to combat the effects of uncomfortable temperatures.

Green and blue space (GBS) is treated as an effective and promising nature-based solution with high efficiency and low cost to contribute to improved thermal comfort [8,9]. Microclimate can be controlled by green spaces through shadowing, evapotranspiration, and photosynthesis [10–12]. Blue spaces form "cool islands" by exchanging air convection due to its greater heat capacity than other materials on the land surface [13–16]. In recent years, evidence of the protective effects of GBSs on heat-related mortality risks was reported [17–19], while several studies have not supported the beneficial associations [20,21]. Speculation of the inconsistent results points to the heterogeneity in landscape composition and configuration regionally and nationally [21]. The ability of GBS to regulate temperature varies with its size, shape, connectivity, and vegetation structure and composition [11,14,22,23], and such features largely depend on the GBS types. Moreover, GBS can alter human outdoor activities [24,25], but little is known about the combined effects of various GBS types on human outdoor activities and heat exposure. Additionally, although low temperatures may triple the risk of high temperatures [26], insufficient attention has been paid to the impacts of GBS on cold-related mortality. The development and implementation of urban greening and blueing strategies require a comprehensive and in-depth understanding and comprehensive quantification of the effects of various GBS types on temperature–health associations.

In the current study, we developed novel exposure indices to reflect the residents' access to overall and type-specific GBS by combining GBS data and fine-scale population distribution data at a small area (i.e., subdistrict) level. This method can reduce the exposure measurement bias or errors by the modifiable areal unit problem (MAUP), which widely exists in prior ecological studies using the area-averaged satellite-based vegetation or water indices. We also assessed the street greenery based on street view images through convolutional neural network models. Then, based on nearly 0.9 million CVD mortality cases, we quantified the effect modifications of GBS in 12 types on both heat- and cold-related CVD mortality risks in 1085 subdistricts in the Zhejiang province of China. Considering GBS management remains far short of type-specific guidelines to combat the health risks of thermal discomfort even in high-income countries, our findings could help decision-makers integrate epidemiological knowledge into their practices and facilitate the development of heat/cold-health action plans to increase resilience to climate change.

2. Methods

2.1. Study area

The study was conducted in Zhejiang, a coastal province in southeastern China, with a subtropical climate characterized by hot, humid summers and cool, dry winters (Fig. 1). Zhejiang is comprised of 11 prefecture-level cities, which include both urban and rural areas. The 11 prefecture-level cities are further divided into 90 districts/counties (termed as districts below), and each district consists of several subdistricts/towns/townships (termed as subdistricts below). Subdistrict was chosen as the analysis unit because it represents the smallest administrative division in the death reporting system. During the study period of 2009–2020, changes in the administrative division of 1365 subdistricts caused the discontinuity of mortality data; thus, we excluded these subdistricts and included 1085 subdistricts for analysis.

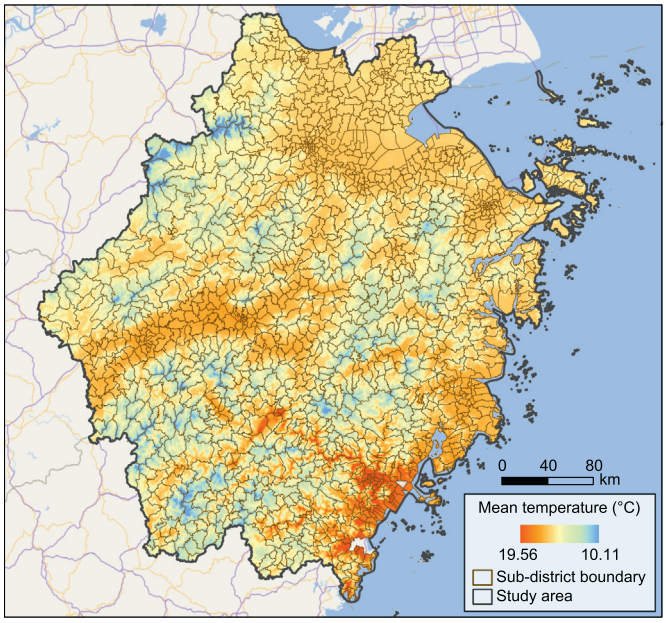

Fig. 1. Location of study area and averaged daily mean temperature during the study period (2009–2020).

2.2. Mortality, demographic, and socioeconomic data

Daily cardiovascular mortality count data during the study period from January 1, 2009 to June 30, 2020 was obtained from the Zhejiang Centre for Disease Control and Prevention based on the National Death Registration Reporting Information System. Subdistrict-specific demographic information on the percentages of old adults (over 65 years) and sex ratios was obtained from the 2010 and 2020 China national census (www.stats.gov.cn/sj/pcsj/rkpc/6rp/indexch.htm, and www.stats.gov.cn/sj/pcsj/rkpc/7rp/indexce.htm). District-specific socioeconomic data on per capita disposable income was obtained from the annual city-level statistical yearbooks (e.g., 2011 Zhejiang Statistical Yearbook [27]).

2.3. Meteorological data

Population-weighted averages of daily 24-h mean temperature and humidity were calculated for each subdistrict to measure human exposure accurately. Hourly temperature and relative humidity observations were obtained from the Zhejiang Meteorological Bureau and collected from a network of 4007 automatic weather stations (AWS) in Zhejiang and neighbouring provinces (Fig. S1). A rigorous automated quality control process was implemented to minimise random errors. Using the global atmospheric reanalysis dataset, the European Centre for Medium-Range Weather Forecast (ECMWF) Interim Re-Analysis (ERA-Interim) [28], hourly temperature and relative humidity data with a spatial resolution of 0.75° was generated. According to a method described in a previous study [29], hourly temperature and humidity were interpolated to a 1 km resolution based on

meteorological observations, ERA-interim, and a digital elevation model (DEM). The five-fold cross-validation showed the method produced accurate prediction with little bias (R^2 = 0.93, $RMSE$ = 0.48 °C).

Population density at a spatial resolution of 1 km was estimated through random forest models [30] based on points-of-interest (POIs), road network, DEM, and multi-source remote sensing data (Fig. 2). The population-weighted averages of daily 24-h mean temperature and humidity for each subdistrict were then calculated using the method previously used by Hu et al. [29].

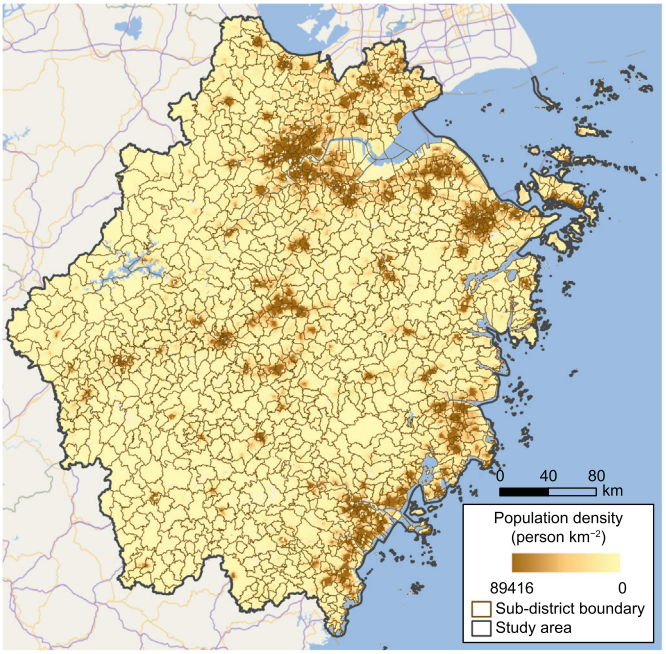

Fig. 2. Population density of all subdistricts in Zhejiang province, China.

2.4. Measurements of green and blue space exposure

We developed exposure indices for each type of GBS to assess subdistrict-level residents' exposure to green and blue spaces. Green spaces were classified into seven types: farms, nature reserves, forests, scrubs, grasses, parks, and street greenery. The exposure indices for farms, nature reserves, forests, scrubs, grasses, and parks were calculated as the ratio of the number of residents living within a buffer zone around a specific type of green space to the total population of a certain subdistrict. Buffer zones were established around the input green space boundaries according to the maximum attraction distance corresponding to different sizes of specified green spaces (Table S1). The boundaries of forests were obtained from Area-of-Interest (AOI) data from the Baidu map (map.baidu.com). The boundaries for other types of green spaces (including farms, nature reserves, forests, scrubs, grasses, and parks) were obtained from OpenStreetMap (www.openstreetmap.org), a collaborative project to create a free global geographic database. Additionally, we applied the method above to calculate the exposure index of overall green spaces, using the buffer zones of patches, including farms, nature reserves, forests, scrubs, grasses, and parks (Fig. 3).

We used the Green View Index (GVI) to measure the green space exposure index for street greenery. We placed sampling points at intervals of 50 m along the road network provided by OpenStreetMap (Fig. 4). Baidu street view images were downloaded from different angles (0°, 90°, 180°, and 270°) at each sampling point between the years 2017 and 2020. Most street view images were collected in the summer when plants and trees are the greenest. A total of 3,314,028 street-view images were gathered from 828,507 sampling points. DeepLab V3+, the third-generation improvement version of Google's DeepLab convolutional neural network series [31], was used to calculate GVI from street view images by semantic segmentation. The xception71_dpc_cityscapes_trainval model was selected, and the CityScapes dataset was used for model training. The average proportion of trees and plants in four matched images was taken as the GVI of each sampling point. The average GVI of all sampling points within a subdistrict

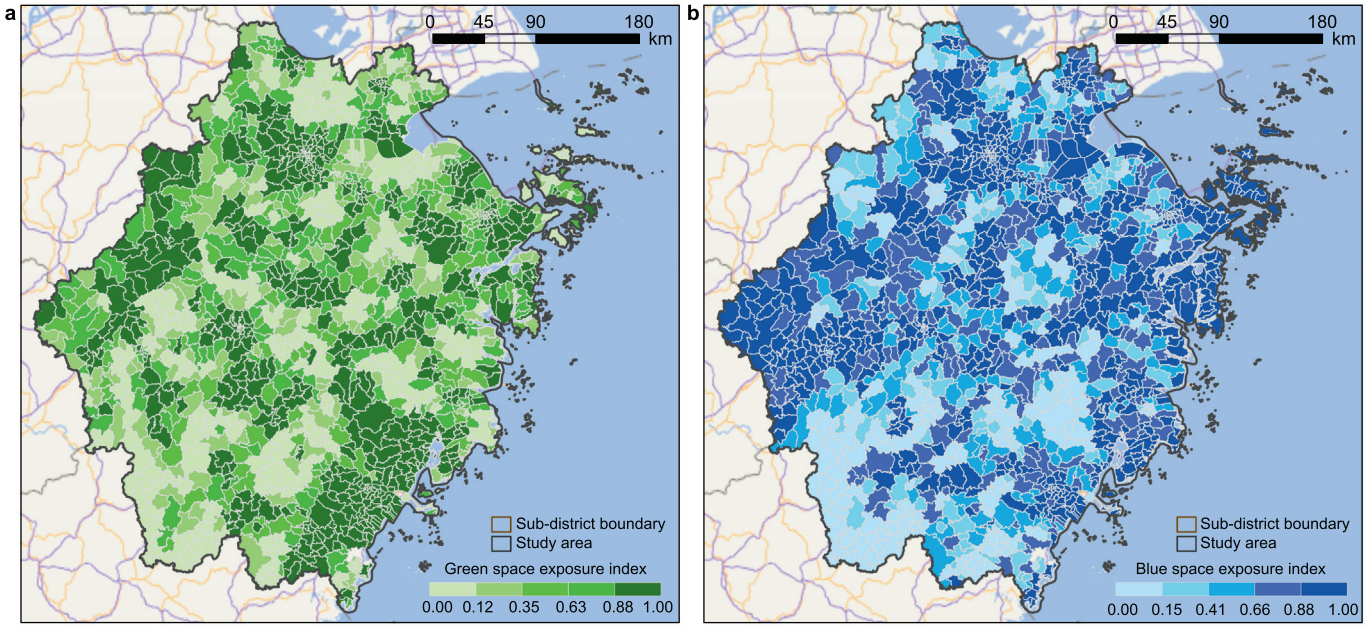

Fig. 3. Subdistrict-level green and blue space exposure indicators: **a**, overall green space exposure index; **b**, overall blue space exposure index.

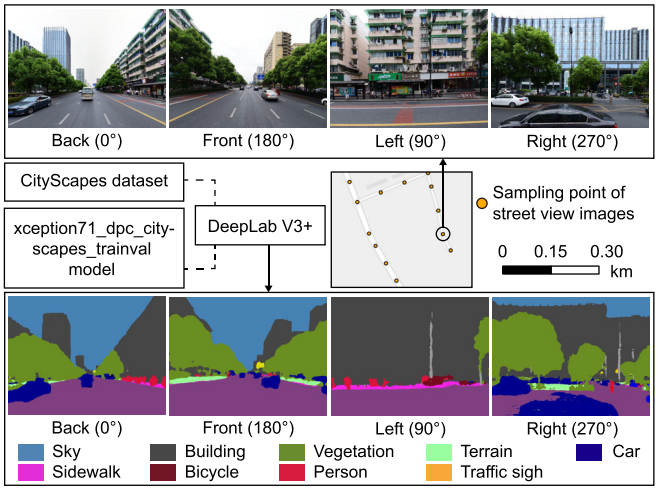

Fig. 4. An example of the sampling point of the street view images and the image segmentation process.

was used to characterise the subdistrict's exposure index of street greenery. The index is between 0 and 1, with higher values indicating higher exposure to street greenery.

Similarly, we classified blue spaces into five types (i.e., lakes, rivers, wetlands, reservoirs, and coasts) [15] and calculated the exposure index for each blue space type. For lakes, rivers, wetlands, reservoirs, and coasts, the blue space exposure index was measured as the ratio of residents living within the buffer zone around a type of blue space to the total population of a certain subdistrict. For inland blue spaces, buffer zones were created around the blue space boundaries according to the maximum attraction distance corresponding to blue space types and sizes (Table S2). For the coast, a 5 km buffer zone was created around the coastline of Zhejiang province [32]. The polygon data of inland blue spaces (i.e., rivers, lakes, wetlands, and reservoirs) were collected from the Chinese river system and river basin dataset (https://www.rserforum.com/thread/212). The exposure index of overall blue spaces was calculated using the buffer zones of all patches of blue spaces (Fig. 3).

2.5. Statistical analysis

A novel case-time series design explored the association between non-optimum temperature and CVD mortality. This design reduced potential biases by aggregating exposures and health outcomes across small geographical areas (e.g., subdistricts) [33]. Temperature-mortality associations at the subdistrict level were estimated through a fixed-effects conditional quasi-Poisson regression with distributed lag non-linear models (DLNMs), which were able to account for both non-linear exposure-response associations and delayed effects [34]. Using strata in the same year, month, and day of the week to match the case and control days within the subdistrict, the regression controlled for long-term and seasonal trends and the day-of-week effect. We then introduced the cross-basis function of daily mean temperature constructed by the DLNM, which included a nature cubic spline with two internal knots at the 33rd and 66th percentiles of the mean temperature distributions [35], as well as a lag response curve with a natural cubic spline with lag knots placed at equally-spaced values along the logarithmic scale [36]. Previous studies have shown that it was inappropriate to use the same exposure lag period for both heat and cold responses, because cold effects often appear several days after exposure and persist for a longer period, whereas heat effects are immediate [37,38]. According to the lag-response associations at high and low temperatures (Fig. S2), we set the maximum lag days for high temperatures as three. We extended the lag days to 21 days to capture the longer delayed effects in cold–mortality associations.

To measure the effect modifications of green and blue spaces on heat- and cold-related mortality risks, a linear interaction between the cross-basis function and the green or blue space exposure index was introduced into the model [33,39]. Relative risks (RRs) of non-optimum temperatures versus (vs.) minimum mortality temperature (MMT) were reported. Temperatures at the 1st, 5th, 10th, 90th, 95th, and 99th percentiles are defined as extreme cold, severe cold, moderate cold, moderate heat, severe heat, and extreme heat, respectively. The ratios of relative risks (RRRs) were calculated using a previously described method [40] to compare RRs between subdistricts with low (P5) and high (P95) levels of green or blue space exposure index. The Z test was used to test the significance of the effect modifications of green and blue spaces [40].

To verify the robustness of our results, sensitivity analyses were conducted by changing the model settings. Firstly, low and high levels of the green and blue space exposure indices were considered to be reset to their respective values at the 10th and 90th percentiles. Secondly, relative humidity at 0–3 lag days was additionally controlled for in the model. In addition, potential confounders, such as the percentage of old adults aged over 65 years, sex ratio, and per capita disposable income, were additionally controlled as the time-varying interactive covariates in the regression models.

All statistical analyses were performed in R software (version 4.2.0), employing the *dlnm, gnm,* and *MASS* packages. The significance level was set at $P < 0.05$ (two-tailed) for all statistical tests.

3. Results

3.1. Descriptive statistics

During a 12-year study period, we observed a total of 902,193 CVD deaths, with an average of 75,183 deaths per year (Table 1). The average mean temperature in Zhejiang province is 16.9 °C, with an average daily relative humidity of 75.9%. The temperatures of extreme heat (P99), severe heat (P95), and moderate heat (P90) were 31.7, 29.3, and 27.7 °C. The temperatures of extreme cold (P1), severe cold (P5), and moderate cold (P10) are −0.5, 2.8, and 5.1 °C, respectively. The mean (SD) values of green space exposure indices were as follows: overall green spaces (0.63 [0.40]), forests (0.57 [0.41]), street greenery (0.06 [0.10]), parks (0.14 [0.28]), nature reserves (0.14 [0.31]), grasses (0.02 [0.12]), farms (0.11 [0.26]), and scrubs (0.02 [0.10]). The mean (SD) values of blue space exposure indices were overall blue spaces (0.70 [0.35]), lakes (0.24 [0.28]), rivers (0.28 [0.37]), reservoirs (0.38 [0.39]), wetlands (0.04 [0.14]), and coasts (0.51 [0.49]).

3.2. Heat-related mortality risks with different types of GBS

For green spaces, subdistricts with high levels of green space exposure to overall green spaces, forests, parks, nature reserves, and street greenery exhibited significantly lower RRs for CVD mortality during extreme heat days (P99) and severe heat days (P95) (Fig. 5). For example, the RR at P95 vs. MMT was higher in subdistricts with a low level of exposure to forests (1.22; 95% CI: 1.19, 1.26) compared to those with a high level of exposure (1.12; 95% CI: 1.09, 1.15), with an estimated RRR of 1.09 (95% CI: 1.05, 1.14) ($P < 0.001$, Table 2). The beneficial effects of higher exposure to overall green spaces, forests, nature reserves, and street greenery were maintained at moderate heat days (P90) ($Ps < 0.01$, Fig. 5);

Table 1
Descriptive statistics of death number and temperature by cities of Zhejiang province, China, for 2009–2020.

City	Number of districts	Number of subdistricts involved	Mean CVD deaths per year	Population-weighted daily mean temperature (°C)[a]
Hangzhou	13	141	10,690	16.9 (−11.0 to 36.0)
Ningbo	10	122	8171	17.2 (−11.3 to 35.6)
Wenzhou	12	100	11,174	17.7 (−7.3 to 33.5)
Shaoxing	6	59	5428	16.6 (−9.8 to 36.2)
Huzhou	5	54	5113	16.7 (−11.3 to 35.9)
Jiaxing	7	63	6078	17.3 (−6.1 to 35.8)
Jinhua	9	141	8298	16.9 (−10.3 to 35.2)
Quzhou	6	96	3772	17.0 (−10.8 to 34.6)
Taizhou	9	111	9830	17.1 (−10.5 to 33.3)
Lishui	9	166	4746	15.8 (−11.0 to 33.8)
Zhoushan	4	32	1883	17.1 (−5.0 to 33.3)
All	90	1085	75,183	16.9 (−11.3 to 36.2)

[a] Mean (min, max).

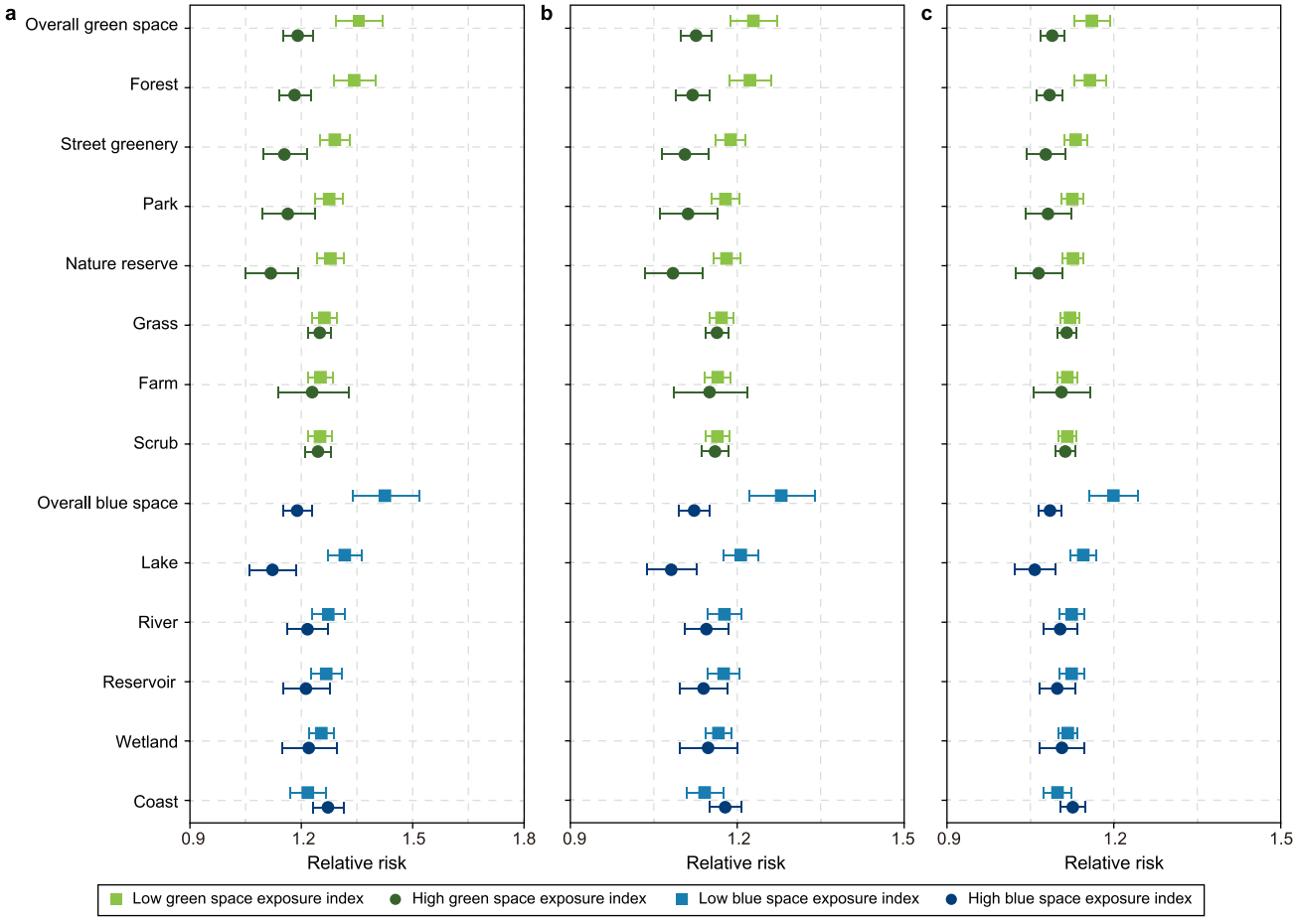

Fig. 5. Relative risk (RR) and its 95% confidence interval (95% CI) of cardiovascular mortality at high temperatures predicted for a subdistrict with a low (light colour) and high (dark colour) value of green and blue space exposure index by green and blue space types. High temperatures: **a**, P99, 31.7 °C; **b**, P95, 29.3 °C; **c**, P90, 27.7 °C.

however, the beneficial effect of parks became insignificant ($P = 0.06$). No effect modification was observed for grasses, farms, or scrubs during either moderate heat, severe heat, or extreme heat days.

For blue spaces, protective associations with heat-related mortality risks during moderate heat, severe heat, and extreme heat days were only observed for overall blue spaces and lakes, but not for rivers, reservoirs, wetlands, and coasts (Fig. 5). For example, the RRs for the population in subdistricts with low and high levels of overall blue space exposure index were 1.28 (95% CI: 1.22, 1.34) and 1.12 (95% CI: 1.10, 1.15) during severe heat days (P95), respectively, with a RRR estimated to be 1.14 (95% CI: 1.08, 1.20) ($P < 0.001$, Table 2). The difference in RRs between high and low levels of blue space exposures to overall blue spaces and lakes gradually became smaller as high temperature decreased from extreme heat to moderate heat (Table 2).

3.3. Cold-related mortality risks with different types of GBS

During extreme cold (P1), severe cold (P5), and moderate cold

Table 2
The ratio of relative risk (RRR) and its 95% confidence interval (95% CI) for cardiovascular mortality at high temperatures (P90, P95, and P99) at high (95%) and low (5%) levels of green and blue space exposure indices and the *Z* test.

Green and blue space type	RRR for a T (27.7 °C) at P90	*P* value	RRR for a T (29.3 °C) at P95	*P* value	RRR for a T (31.7 °C) at P99	*P* value
Green space type						
Overall	**1.07 (1.03, 1.10)**	**<0.001**	**1.09 (1.05, 1.14)**	**<0.001**	**1.14 (1.07, 1.21)**	**<0.001**
Forest	**1.07 (1.03, 1.10)**	**<0.001**	**1.09 (1.05, 1.14)**	**<0.001**	**1.14 (1.07, 1.20)**	**<0.001**
Street greenery	**1.05 (1.01, 1.09)**	**<0.01**	**1.07 (1.03, 1.12)**	**<0.01**	**1.12 (1.05, 1.19)**	**<0.001**
Park	1.04 (1.00, 1.08)	0.060	**1.06 (1.01, 1.12)**	**<0.05**	**1.10 (1.02, 1.17)**	**<0.01**
Nature reserve	**1.06 (1.01, 1.10)**	**<0.01**	**1.09 (1.03, 1.15)**	**<0.01**	**1.14 (1.07, 1.23)**	**<0.001**
Grass	1.01 (0.98, 1.03)	0.634	1.01 (0.98, 1.03)	0.605	1.01 (0.97, 1.05)	0.584
Farm	1.01 (0.96, 1.06)	0.708	1.01 (0.95, 1.08)	0.685	1.02 (0.94, 1.11)	0.669
Scrub	1.00 (0.98, 1.03)	0.785	1.00 (0.98, 1.03)	0.795	1.00 (0.97, 1.04)	0.811
Blue space type						
Overall	**1.11 (1.06, 1.15)**	**<0.001**	**1.14 (1.08, 1.20)**	**<0.001**	**1.20 (1.12, 1.29)**	**<0.001**
Lake	**1.08 (1.04, 1.13)**	**<0.001**	**1.12 (1.06, 1.17)**	**<0.001**	**1.17 (1.10, 1.25)**	**<0.001**
River	1.02 (0.98, 1.05)	0.295	1.03 (0.99, 1.07)	0.195	1.05 (0.99, 1.11)	0.125
Reservoir	1.02 (0.99, 1.06)	0.196	1.03 (0.99, 1.08)	0.171	1.05 (0.98, 1.11)	0.157
Wetland	1.01 (0.97, 1.05)	0.636	1.02 (0.97, 1.07)	0.517	1.03 (0.96, 1.10)	0.410
Coast	0.98 (0.95, 1.01)	0.107	0.97 (0.93, 1.01)	0.097	0.96 (0.91, 1.01)	0.095

Note:
(1) RRR refers to the ratio of RR at the 90th, 95th, or 99th percentiles of the temperature compared to MMT at high (95%) and low (5%) levels of green and blue space exposure indices.
(2) *P* value refers to the significance of the difference between the RRs at the 90th, 95th, or 99th percentiles of the temperature compared to MMT at high (95%) and low (5%) levels of green and blue space exposure indices using *Z* test.

(P10) days, significantly lower cold-related CVD mortality risks were found in subdistricts with higher levels of blue space exposures to rivers and coasts (Fig. 6), rather than to other blue space types of overall blue spaces, lakes, wetlands, and reservoirs, as well as all types of green spaces. For example, the RRs at P1 vs. MMT were higher for the population in subdistricts with a low exposure

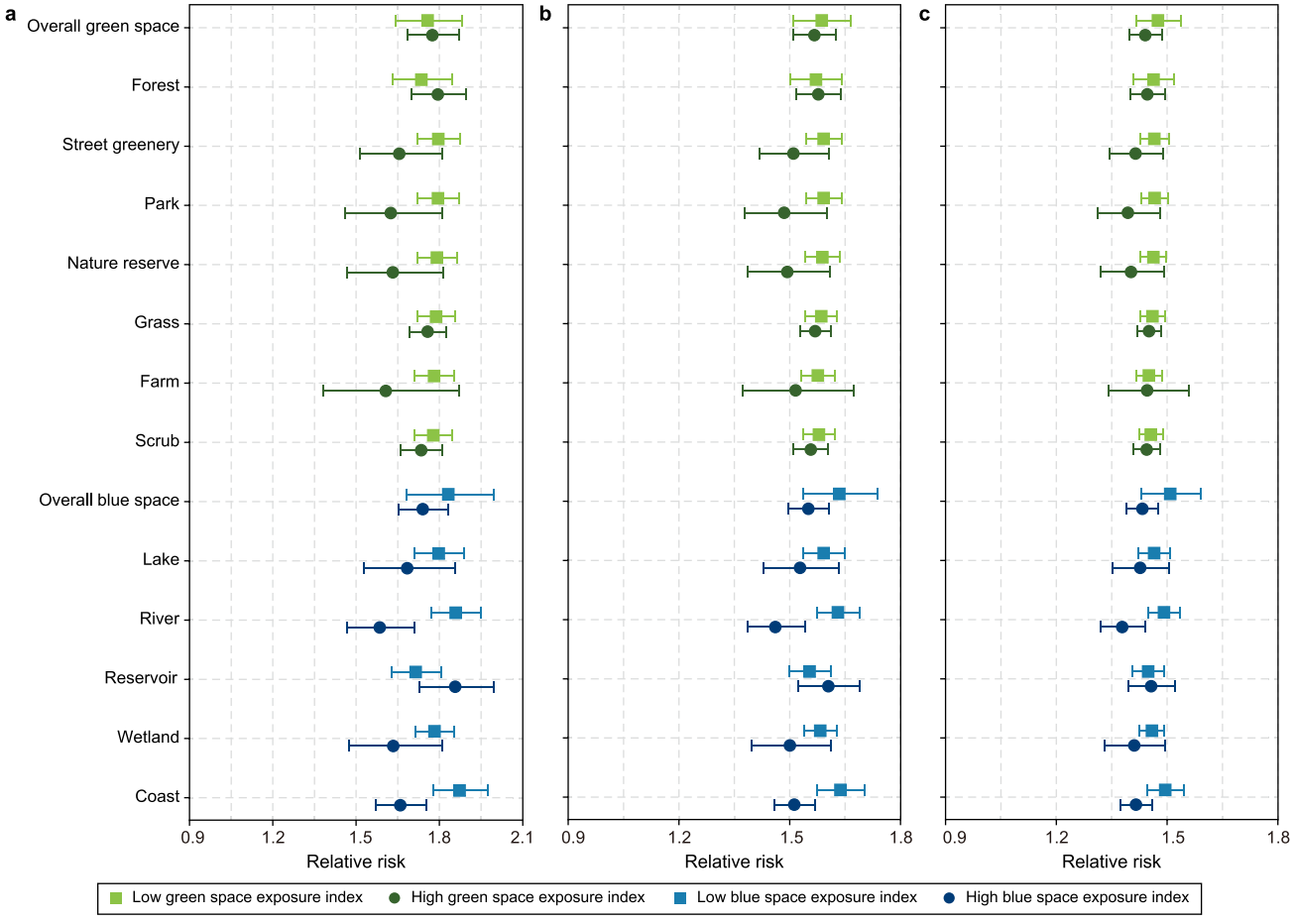

Fig. 6. Relative risk (RR) and its 95% confidence interval (95% CI) of cardiovascular mortality at low temperatures predicted for a subdistrict with a low (light colour) and high (dark colour) value of green and blue space exposure index by green and blue space types. Low temperatures: **a**, P1, −0.5 °C; **b**, P5, 2.8 °C; **c**, P10, 5.1 °C.

Table 3
The ratio of relative risk (RRR) and its 95% confidence interval (95% CI) for cardiovascular mortality at low temperatures (P10, P5, and P1) at high (95%) and low (5%) levels of green and blue space exposure indices and the *Z* test.

Green and blue space type	RRR for a T (5.1 °C) at P10	*P* value	RRR for a T (2.8 °C) at P5	*P* value	RRR for a T (−0.5 °C) at P1	*P* value
Green space type						
Overall	1.02 (0.97, 1.08)	0.367	1.01 (0.95, 1.08)	0.690	0.99 (0.91, 1.08)	0.828
Forest	1.01 (0.96, 1.06)	0.640	1.00 (0.94, 1.06)	0.894	0.97 (0.89, 1.05)	0.429
Street greenery	1.04 (0.98, 1.10)	0.226	1.05 (0.98, 1.13)	0.137	1.08 (0.98, 1.20)	0.110
Park	1.05 (0.99, 1.12)	0.131	1.07 (0.99, 1.16)	0.089	1.10 (0.98, 1.24)	0.090
Nature reserve	1.04 (0.98, 1.11)	0.210	1.06 (0.98, 1.15)	0.131	1.10 (0.98, 1.23)	0.107
Grass	1.01 (0.98, 1.04)	0.696	1.01 (0.97, 1.05)	0.593	1.02 (0.96, 1.07)	0.531
Farm	1.00 (0.93, 1.09)	0.933	1.04 (0.94, 1.15)	0.459	1.11 (0.95, 1.30)	0.199
Scrub	1.01 (0.97, 1.04)	0.652	1.01 (0.97, 1.06)	0.496	1.03 (0.97, 1.09)	0.398
Blue space type						
Overall	1.05 (0.99, 1.12)	0.097	1.05 (0.98, 1.13)	0.148	1.05 (0.95, 1.16)	0.309
Lake	1.03 (0.97, 1.09)	0.406	1.04 (0.97, 1.12)	0.292	1.07 (0.96, 1.19)	0.245
River	**1.08 (1.03, 1.14)**	**<0.01**	**1.12 (1.05, 1.19)**	**<0.001**	**1.17 (1.07, 1.28)**	**<0.001**
Reservoir	0.99 (0.94, 1.05)	0.832	0.97 (0.91, 1.03)	0.316	0.92 (0.85, 1.01)	0.077
Wetland	1.03 (0.97, 1.10)	0.294	1.05 (0.98, 1.14)	0.168	1.09 (0.98, 1.22)	0.118
Coast	**1.06 (1.01, 1.10)**	**<0.05**	**1.08 (1.03, 1.14)**	**<0.01**	**1.13 (1.05, 1.22)**	**<0.01**

Note:
(1) RRR refers to the ratio of RR at the 10th, 5th, or 1st percentiles of the temperature compared to MMT at high (95%) and low (5%) levels of green and blue space exposure indices.
(2) *P* value refers to the significance of the difference between the RRs at the 10th, 5th, or 1st percentiles of the temperature compared to MMT at high (95%) and low (5%) levels of green and blue space exposure indices using the *Z* test.

level of rivers (1.86; 95% CI: 1.77, 1.95) than those with a high exposure level of rivers (1.59; 95% CI: 1.47, 1.71). The corresponding RRR was estimated to be 1.17 (95% CI: 1.07, 1.28) ($P < 0.001$, Table 3), indicating a distinct disparity between subdistricts with high and low exposure levels of rivers.

3.4. Sensitivity analyses

In the sensitivity analyses, we found robust effect modifications of specific types of green and blue spaces after using different definitions of the high and low levels of green and blue space exposure indices or additionally adjusting for confounders including humidity, percentage of people aged over 65 years, sex, and income in the model (Figs. S3–12).

4. Discussion

To our knowledge, this study is the first to provide epidemiological insights into the complexity of effect modifications of different types of GBS on both heat- and cold-related CVD mortality risks. Based on the small-area analysis of 1085 subdistricts in Zhejiang province, China, we found that higher exposure to certain types of GBS, including forests, parks, nature reserves, street greenery, and lakes, could alleviate the risk of heat-related CVD mortality. For cold-related CVD mortality, only blue space types of rivers and coasts showed significant protective effects. Our findings highlight the effectiveness of certain GBS types in mitigating the mortality risks associated with non-optimum temperatures.

The cooling effects of all green space types in the warm season are well established [41]. However, we only observed significant mitigation of heat-induced mortality for a few types of green spaces. The major reason may be related to the distinction of patch size. Various city case studies have reported that larger green spaces (e.g., forests, nature reserves, and parks) contributed to greater cooling effects [16,42,43]. Another potential explanation is the varying cooling effects of different vegetation structures [16]. A lack of tree canopy to absorb shortwave radiation can lead to a high vapour pressure deficit, which triggers a physiological reaction that causes stomatal closure and hinders transpiration cooling [44]. Meanwhile, the underlying ground vegetation beneath the tree canopy shades does not get adequate radiation for transpiration [22]. Forests, parks, nature reserves, and street greenery often have dense, extensive canopy cover with multi-layered vegetation structures. They can provide stronger cooling effects than grasses, farms, and scrubs.

Decreased cooling capacity in winter may lead to no apparent impact of all green space types on cold-related CVD mortality in Zhejiang. This phenomenon could be regarded as a verification of the findings by Hathway and Sharples [45], Schatz and Kucharik [46], and Solcerova et al. [47], who reported a stronger cooling effect of green spaces in summer than in winter. The cooling effects of green spaces are mainly obtained by sensible and latent heat reduction. Seasonal sensible heat flux was found to be lowest during the winter, while the highest heat flux occurs in the summer season when the vegetation-to-atmosphere temperature gradient is higher [15] — so that in winter green spaces (e.g., forests) in some climate zones have moderate warming effects [15]. Besides, past evidence showed stronger cooling during the daytime in summer but stronger cooling of vegetation during the night in winter [41]. Indeed, cold exposure for the population at night is likely mainly driven by the indoor environment. It is, therefore, unlikely that the actual temperature exposure of residents during the winter will be greatly affected by the cooling of green spaces.

Among all blue space types, only the lakes were observed to mitigate the heat-related CVD mortality risks, despite this benefit being larger than any type of green spaces. For rivers, reservoirs, and wetlands, the cooling intensity of their waterbody patches may be weaker than those of lakes since larger size and compact shape of waterbodies can reduce temperature better than smaller sizes and elongated or irregular shapes, respectively [14,48,49]. Despite the vast expanse of oceans compared to inland water bodies, the evaporation of seawater may raise the air humidity and consequently offset the benefits of thermal comfort [49]. Further, consistent with a study by Song et al. [21] in Hong Kong, the non-significant mitigation effect of the coast was also speculated to be partly explained by the fact that the coastal populations are far more likely to engage in outdoor physical activities or works than the non-coastal populations during heat waves [25,50].

During the cold season, only rivers and coastal areas exhibited protective effects against cold-related health issues. The benefits of residing near the coast can be naturally explained by the warming effect of the ocean [13,15]. As solar radiation decreases in winter,

the ocean can gradually release the stored heat and warm the coastal areas [15]. Meanwhile, we cannot rule out the influence of better health status of people living near the coast potentially benefiting from enhanced physical activity [25]. Among all types of inland blue spaces, no significant modification of effects was observed for lakes, wetlands, or reservoirs. Prior studies that tried to assess the impact of waterbodies found that lakes, wetlands, and reservoirs can provide warming as rivers during the winter [45,51]. The underlying reason for the discrepancy in the impacts of different inland blue space types on cold-induced CVD mortality is still unknown and needs further exploration.

Our findings reinforce the greening and blueing strategy in urban development and renewal as an effective adaptation policy to climate change. Results support that the trade-offs between potentially enhanced outdoor activities due to green spaces (e.g., urban parks, street greenery) and the cooling effects yield net protective effects against temperature-related mortality. It lessens the worries about the increased health risks from higher exposure time to outdoor non-optimum temperatures due to more visits to public green spaces. Concrete ways to achieve a climate-resilient development of green space planning for a healthy city include preserving forests and nature reserves, improving spatial equity of urban parks, and increasing street greenery. Creating new blue space is difficult in most developed areas, but developing conservation actions to protect the rivers and lakes around neighbourhoods should be recommended. In addition, our study confirmed that disparity in temperature-related mortality is partially attributed to the inequality of access to certain GBS types. Accordingly, indicators of insufficient neighbourhood GBS should be included in future vulnerability assessment models. The inclusion should also consider the varying effects at different temperatures.

The current study benefited from (a) the use of an advanced case-time series design to assess GBS exposures in small geographical areas to reduce the exposure assessment bias and errors from MAUP; (b) the application of novel GBS exposure indices considering both size and distance to the residences of the GBS, as well as the exposure index of street greenery based on a large sample of street view images through machine learning techniques. Nonetheless, several limitations should be acknowledged. First, temperature-related mortality risks are largely affected by various individual factors, such as the use of air conditioning and heating [52,53]. Although we carefully attempted to test potential confounding effects (e.g., age, sex, income), residual confounding cannot be fully ruled out. Second, despite the interaction effects of air pollution (e.g., particulate matter, ozone) and temperature on mortality previously reported [54], air pollution was not included in our analysis due to the data unavailability for the entire study period. Third, GBS exposure assessments were based on the assumption that the willingness to visit GBS for the exposed population is the same in different subdistricts without accounting for human time-activity patterns, which are worth considering in further research. Additionally, prior studies have demonstrated that the cooling effects of GBS vary by local background climate [41]. Therefore, there is uncertainty about the extrapolation of our results to other regions and countries. Finally, the income data used in the sensitivity analysis were collected at the district level rather than the subdistrict level because subdistrict-level data were not publicly available. This may reduce the ability to detect the impact of the potential confounding effects of income on the effect modification of GBS.

Conclusions

Green and blue spaces have significant protective effects on CVD mortality at high temperatures in Zhejiang province, China, whereas only blue spaces showed protective effects at low temperatures. Specifically, higher exposures to forests, parks, nature reserves, street greenery, and lakes are associated with a decreased risk of heat-related CVD mortality, while higher exposures to rivers and coasts are associated with a decreased risk of cold-related CVD mortality. Notably, blue spaces confer greater protective benefits than green spaces, with these benefits intensifying alongside more extreme temperature conditions. Our findings provide a deeper understanding of the linkage of type-specific GBS and health risks attributable to non-optimum temperatures, providing insights for decision-makers to obtain the maximum health benefits of GBS in actionable climate adaptation planning.

CRediT authorship contribution statement

Kejia Hu: Formal Analysis, Investigation, Conceptualization, Methodology, Software, Writing - Original Draft, Writing - Review & Editing. **Shiyi Wang:** Data Curation, Visualization, Investigation, Writing - Review & Editing. **Fangrong Fei:** Data Curation, Supervision. **Jinglu Song:** Methodology. **Feng Chen:** Data Curation, Writing - Review & Editing. **Qi Zhao:** Methodology. **Yujie Shen:** Data Curation. **Jingqiao Fu:** Data Curation, Validation. **Yunquan Zhang:** Methodology. **Jian Cheng:** Methodology. **Jieming Zhong:** Supervision, Methodology, Writing - Review & Editing. **Xuchao Yang:** Supervision, Funding Acquisition, Methodology, Writing - Review & Editing. **Jiayu Wu:** Supervision, Funding Acquisition, Conceptualization, Writing - Review & Editing.

Declaration of competing interest

The authors declare that they have no known competing financial interests or personal relationships that could have appeared to influence the work reported in this paper.

Acknowledgements

The study was supported by the National Natural Science Foundation of China (42001013, 41971019, 32271935), the Zhejiang Provincial Natural Science Foundation of China (Y23D050006), the Key Laboratory of Intelligent Preventive Medicine of Zhejiang Province, China (2020E10004), the Leading Innovative and Entrepreneur Team Introduction Program of Zhejiang (2019R01007), and the Healthy Zhejiang One Million People Cohort (20230085).

Appendix A. Supplementary data

Supplementary data to this article can be found online at https://doi.org/10.1016/j.ese.2024.100408.

References

[1] G.A. Roth, G.A. Mensah, C.O. Johnson, et al., Global burden of cardiovascular diseases and risk factors, 1990–2019, J. Am. Coll. Cardiol. 76 (2020) 2982–3021, https://doi.org/10.1016/j.jacc.2020.11.010.
[2] S. Gu, L. Zhang, S. Sun, et al., Projections of temperature-related cause-specific mortality under climate change scenarios in a coastal city of China, Environ. Int. 143 (2020) 105889, https://doi.org/10.1016/j.envint.2020.105889.
[3] B. Alahmad, H. Khraishah, D. Royé, et al., Associations between extreme temperatures and cardiovascular cause-specific mortality: results from 27 countries, Circulation 147 (2023) 35–46, https://doi.org/10.1161/CIRCULATIONAHA.122.061832.
[4] S. Al-Kindi, I. Motairek, H. Khraishah, S. Rajagopalan, Cardiovascular disease burden attributable to non-optimal temperature: analysis of the 1990–2019 global burden of disease, European Journal of Preventive Cardiology (2023), https://doi.org/10.1093/eurjpc/zwad130.
[5] Q. Xing, Z. Sun, Y. Tao, et al., Projections of future temperature-related cardiovascular mortality under climate change, urbanization and population aging in Beijing, China. Environment International. 163 (2022) 107231, https://doi.org/10.1016/j.envint.2022.107231.

[6] J. Yang, M. Zhou, Z. Ren, et al., Projecting heat-related excess mortality under climate change scenarios in China, Nat. Commun. 12 (2021) 1039, https://doi.org/10.1038/s41467-021-21305-1.
[7] A. Gasparrini, Y. Guo, F. Sera, et al., Projections of temperature-related excess mortality under climate change scenarios, Lancet Planet. Health 1 (2017) e360–e367, https://doi.org/10.1016/S2542-5196(17)30156-0.
[8] C.W. McDougall, N. Hanley, R.S. Quilliam, D.M. Oliver, Blue space exposure, health and well-being: does freshwater type matter? Landsc. Urban Plann. 224 (2022) 104446 https://doi.org/10.1016/j.landurbplan.2022.104446.
[9] D. Rojas-Rueda, M.J. Nieuwenhuijsen, M. Gascon, D. Perez-Leon, P. Mudu, Green spaces and mortality: a systematic review and meta-analysis of cohort studies, Lancet Planet. Health 3 (2019) e469–e477, https://doi.org/10.1016/S2542-5196(19)30215-3.
[10] H. Akbari, M. Pomerantz, H. Taha, Cool surfaces and shade trees to reduce energy use and improve air quality in urban areas, Sol. Energy 70 (2001) 295–310, https://doi.org/10.1016/S0038-092X(00)00089-X.
[11] N. Meili, G. Manoli, P. Burlando, et al., Tree effects on urban microclimate: diurnal, seasonal, and climatic temperature differences explained by separating radiation, evapotranspiration, and roughness effects, Urban For. Urban Green. 58 (2021) 126970, https://doi.org/10.1016/j.ufug.2020.126970.
[12] S.-S. Peng, S. Piao, Z. Zeng, et al., Afforestation in China cools local land surface temperature, Proc. Natl. Acad. Sci. USA 111 (2014) 2915–2919, https://doi.org/10.1073/pnas.1315126111.
[13] P. Ampatzidis, T. Kershaw, A review of the impact of blue space on the urban microclimate, Sci. Total Environ. 730 (2020) 139068, https://doi.org/10.1016/j.scitotenv.2020.139068.
[14] H. Du, X. Song, H. Jiang, Z. Kan, Z. Wang, Y. Cai, Research on the cooling island effects of water body: a case study of Shanghai, China, Ecol. Indicat. 67 (2016) 31–38, https://doi.org/10.1016/j.ecolind.2016.02.040.
[15] K.R. Gunawardena, M.J. Wells, T. Kershaw, Utilising green and bluespace to mitigate urban heat island intensity, Sci. Total Environ. 584–585 (2017) 1040–1055, https://doi.org/10.1016/j.scitotenv.2017.01.158.
[16] M. Vaz Monteiro, K.J. Doick, P. Handley, A. Peace, The impact of greenspace size on the extent of local nocturnal air temperature cooling in London, Urban For. Urban Green. 16 (2016) 160–169, https://doi.org/10.1016/j.ufug.2016.02.008.
[17] K. Burkart, F. Meier, A. Schneider, et al., Modification of heat-related mortality in an elderly urban population by vegetation (urban green) and proximity to water (urban blue): evidence from Lisbon, Portugal, Environmental Health Perspectives 124 (2016) 927–934, https://doi.org/10.1289/ehp.1409529.
[18] H.M. Choi, W. Lee, D. Roye, et al., Effect modification of greenness on the association between heat and mortality: a multi-city multi-country study, EBioMedicine 84 (2022), https://doi.org/10.1016/j.ebiom.2022.104251.
[19] M. Pascal, S. Goria, V. Wagner, et al., Greening is a promising but likely insufficient adaptation strategy to limit the health impacts of extreme heat, Environ. Int. 151 (2021) 106441, https://doi.org/10.1016/j.envint.2021.106441.
[20] J.-Y. Son, K.J. Lane, J.-T. Lee, M.L. Bell, Urban vegetation and heat-related mortality in Seoul, Korea, Environ. Res. 151 (2016) 728–733, https://doi.org/10.1016/j.envres.2016.09.001.
[21] J. Song, Y. Lu, Q. Zhao, et al., Effect modifications of green space and blue space on heat–mortality association in Hong Kong, Sci. Total Environ. 838 (2008–2017) 156127, https://doi.org/10.1016/j.scitotenv.2022.156127, 2022.
[22] M.A. Rahman, A. Moser, T. Rötzer, S. Pauleit, Comparing the transpirational and shading effects of two contrasting urban tree species, Urban Ecosyst. 22 (2019) 683–697, https://doi.org/10.1007/s11252-019-00853-x.
[23] R. Sun, L. Chen, How can urban water bodies be designed for climate adaptation? Landsc. Urban Plann. 105 (2012) 27–33, https://doi.org/10.1016/j.landurbplan.2011.11.018.
[24] I. Markevych, J. Schoierer, T. Hartig, et al., Exploring pathways linking greenspace to health: theoretical and methodological guidance, Environ. Res. 158 (2017) 301–317, https://doi.org/10.1016/j.envres.2017.06.028.
[25] T.P. Pasanen, M.P. White, B.W. Wheeler, J.K. Garrett, L.R. Elliott, Neighbourhood blue space, health and wellbeing: the mediating role of different types of physical activity, Environ. Int. 131 (2019) 105016, https://doi.org/10.1016/j.envint.2019.105016.
[26] H. Liu, M. Tong, F. Guo, et al., Deaths attributable to anomalous temperature: a generalizable metric for the health impact of global warming, Environ. Int. 169 (2022) 107520, https://doi.org/10.1016/j.envint.2022.107520.
[27] Zhejiang statistical yearbook [internet]. Zhejiang provincial Bureau of statistics. http://tjj.zj.gov.cn/col/col1525563/index.html, 2011. (Accessed 20 March 2023).
[28] D.P. Dee, S.M. Uppala, A.J. Simmons, et al., The ERA-Interim reanalysis: configuration and performance of the data assimilation system, Q. J. R. Meteorol. Soc. 137 (2011) 553–597, https://doi.org/10.1002/qj.828.
[29] K. Hu, Y. Guo, S. Hochrainer-Stigler, et al., Evidence for urban–rural disparity in temperature–mortality relationships in Zhejiang province, China, Environmental Health Perspectives 127 (2019) 037001, https://doi.org/10.1289/EHP3556.
[30] T. Ye, N. Zhao, X. Yang, et al., Improved population mapping for China using remotely sensed and points-of-interest data within a random forests model, Sci. Total Environ. 658 (2019) 936–946, https://doi.org/10.1016/j.scitotenv.2018.12.276.
[31] Encoder-decoder with atrous separable convolution for semantic image segmentation, in: L.-C. Chen, Y. Zhu, G. Papandreou, F. Schroff, H. Adam (Eds.), Proceedings of the European Conference on Computer Vision, ECCV), 2018.
[32] A. Hooyberg, H. Roose, J. Grellier, et al., General health and residential proximity to the coast in Belgium: results from a cross-sectional health survey, Environ. Res. 184 (2020) 109225, https://doi.org/10.1016/j.envres.2020.109225.
[33] A. Gasparrini, P. Masselot, M. Scortichini, et al., Small-area assessment of temperature-related mortality risks in England and Wales: a case time series analysis, Lancet Planet. Health 6 (2022) e557–e564, https://doi.org/10.1016/S2542-5196(22)00138-3.
[34] A. Gasparrini, B. Armstrong, M.G. Kenward, Distributed lag non-linear models, Stat. Med. 29 (2010) 2224–2234, https://doi.org/10.1002/sim.3940.
[35] R. Pan, Y. Honda, E. Minakuchi, E. Kim Satbyul, M. Hashizume, Y. Kim, Ambient temperature and external causes of death in Japan from 1979 to 2015: a time-stratified case-crossover analysis, Environmental Health Perspectives 130 (2022) 047004, https://doi.org/10.1289/EHP9943.
[36] Y. Guo, A. Gasparrini, B. Armstrong, et al., Global variation in the effects of ambient temperature on mortality: a systematic evaluation, Epidemiology 25 (2014) 781, https://doi.org/10.1097/EDE.0000000000000165.
[37] J. Huang, J. Wang, W. Yu, The lag effects and vulnerabilities of temperature effects on cardiovascular disease mortality in a subtropical climate zone in China, Int. J. Environ. Res. Publ. Health 11 (2014) 3982–3994, https://doi.org/10.3390/ijerph110403982.
[38] W. Yu, W. Hu, K. Mengersen, et al., Time course of temperature effects on cardiovascular mortality in Brisbane, Australia, Heart 97 (2011) 1089, https://doi.org/10.1136/hrt.2010.217166.
[39] A. Gasparrini, A tutorial on the case time series design for small-area analysis, BMC Med. Res. Methodol. 22 (2022) 129, https://doi.org/10.1186/s12874-022-01612-x.
[40] D.G. Altman, J.M. Bland, Interaction revisited: the difference between two estimates, BMJ 326 (2003) 219, https://doi.org/10.1136/bmj.326.7382.219.
[41] Z. Yu, G. Yang, S. Zuo, G. Jørgensen, M. Koga, H. Vejre, Critical review on the cooling effect of urban blue-green space: a threshold-size perspective, Urban For. Urban Green. 49 (2020) 126630, https://doi.org/10.1016/j.ufug.2020.126630.
[42] D.E. Bowler, L. Buyung-Ali, T.M. Knight, A.S. Pullin, Urban greening to cool towns and cities: a systematic review of the empirical evidence, Landsc. Urban Plann. 97 (2010) 147–155, https://doi.org/10.1016/j.landurbplan.2010.05.006.
[43] C.-R. Chang, M.-H. Li, S.-D. Chang, A preliminary study on the local cool-island intensity of Taipei city parks, Landsc. Urban Plann. 80 (2007) 386–395, https://doi.org/10.1016/j.landurbplan.2006.09.005.
[44] J.I.L. Morison, R.M. Gifford, Stomatal sensitivity to carbon dioxide and humidity: a comparison of two C3 and two C4 grass species, Plant Physiology 71 (1983) 789–796, https://doi.org/10.1104/pp.71.4.789.
[45] E.A. Hathway, S. Sharples, The interaction of rivers and urban form in mitigating the Urban Heat Island effect: a UK case study, Build. Environ. 58 (2012) 14–22, https://doi.org/10.1016/j.buildenv.2012.06.013.
[46] J. Schatz, C.J. Kucharik, Urban heat island effects on growing seasons and heating and cooling degree days in Madison, Wisconsin USA, Int. J. Climatol. 36 (2016) 4873–4884, https://doi.org/10.1002/joc.4675.
[47] A. Solcerova, F. van de Ven, M. Wang, M. Rijsdijk, N. van de Giesen, Do green roofs cool the air? Build. Environ. 111 (2017) 249–255, https://doi.org/10.1016/j.buildenv.2016.10.021.
[48] J. Peng, Q. Liu, Z. Xu, et al., How to effectively mitigate urban heat island effect? A perspective of waterbody patch size threshold, Landsc. Urban Plann. 202 (2020) 103873, https://doi.org/10.1016/j.landurbplan.2020.103873.
[49] N.E. Theeuwes, A. Solcerová, G.J. Steeneveld, Modeling the influence of open water surfaces on the summertime temperature and thermal comfort in the city, J. Geophys. Res. Atmos. 118 (2013) 8881–8896, https://doi.org/10.1002/jgrd.50704.
[50] M.P. White, B.W. Wheeler, S. Herbert, I. Alcock, M.H. Depledge, Coastal proximity and physical activity: is the coast an under-appreciated public health resource? Prev. Med. 69 (2014) 135–140, https://doi.org/10.1016/j.ypmed.2014.09.016.
[51] A.N. Moyer, T.W. Hawkins, River effects on the heat island of a small urban area, Urban Clim. 21 (2017) 262–277, https://doi.org/10.1016/j.uclim.2017.07.004.
[52] A.G. Barnett, Temperature and cardiovascular deaths in the US elderly: changes over time, Epidemiology 18 (2007), https://doi.org/10.1097/01.ede.0000257515.34445.a0.
[53] K. Chen, L. Zhou, X. Chen, et al., Urbanization level and vulnerability to heat-related mortality in jiangsu province, China, Environmental Health Perspectives 124 (2016) 1863–1869, https://doi.org/10.1289/EHP204.
[54] L.-Y. Ma, W.-W. Chen, R.-L. Gao, et al., China cardiovascular diseases report 2018: an updated summary, Journal of geriatric cardiology: JGC 17 (2020) 1, https://doi.org/10.11909/j.issn.1671-5411.2020.01.001.